NASA Technical Paper 1797

Sample Data Effects of High-Pass Filters

David O. Chin

JANUARY 1981

NASA

NASA Technical Paper 1797

Sample Data Effects of High-Pass Filters

David O. Chin
Ames Research Center
Moffett Field, California

National Aeronautics
and Space Administration

**Scientific and Technical
Information Branch**

1981

SYMBOLS

$H(s)$	Laplace transfer function of continuous filter
$H(z)$	Z-transform of H(s)
j	imaginary operator, $\sqrt{-1}$
n	ω_s/ω_n, normalized sample frequency or discrete time index
s	Laplace variable
T	sample period, sec
$U(s)$	Laplace transform of u
u	continuous input variable
$Y(s)$	Laplace transform of y
y	continuous output variable
Z	Z-transform operator
z	Z-transform variable
ζ	damping ratio of second-order model
τ	time constant, sec
ω	frequency of sinusoidal input variable, rad/sec
ω_c	corner frequency of first-order high-pass filter, rad/sec
ω_n	umdamped natural frequency of second-order model, rad/sec
ω_s	frequency of computation or sampling, rad/sec
$(\dot{})$	time derivative
$\Big\vert_{s\,=}$	function evaluated at s =

SAMPLE DATA EFFECTS OF HIGH-PASS FILTERS

David O. Chin
Ames Research Center

SUMMARY

The fact that aircraft motion simulators inherently have less travel than the actual aircraft being simulated has resulted in the application of digital washout filters in the computer software. Four commonly used mathematical models of linear first- and second-order high-pass washout filters were analyzed. These models were Euler's Integration, Zero-Order Hold, Bilinear Transformation, and Second-Order Adams-Bashforth Integration. Bode responses for each model at various sample rates were compared to the continuous filter response. The results show that higher sample rates produce Bode responses approaching the continuous response and the Bilinear Transformation model produced the best responses over the frequency spectrum and sample rates. Pole location analysis of each model in the z-plane shows the Bilinear Transformation and Zero-Order Hold models gave stable poles regardless of time step size, whereas the other models did not always display stable poles.

A near constant gain error over the entire frequency spectrum was discovered in the Zero-Order Hold cases and a correction gain was calculated for the first-order high-pass filter case.

INTRODUCTION

One of the continuing areas of research in real-time man-in-the-loop aircraft simulations is simulator motion recovery. The fact that motion simulators have less travel than the aircraft being simulated results in compromises in the motion felt by the simulator pilot. In an attempt to utilize the limited travel most effectively, low-frequency portions of the motion signals are eliminated with "washout filters."

Washout filters are merely high-pass filters and can be implemented digitally by any number of mathematical models which approximate continuous filters. This study examines the effects of modeling a linear first- and second-order high-pass filter with four commonly used models. The models are: Euler's Integration, Zero-Order Hold (ZOH), Bilinear Transformation (Tustin's Approximation), and Second-Order Adams-Bashforth Integration.

As a means of comparison, the frequency responses for each mathematical model are analyzed against the continuous filter response while varying the sample rate. The z-plane pole locations of each model are also analyzed for stability.

HIGH-PASS FILTER MODELS

To obtain the Bode plots for comparing the various mathematical models, the mathematical representations of the first- and second-order high-pass filters are needed.

First-Order High-Pass Filter

The first-order high-pass filter (FOHP) is defined as:

$$\dot{y} + \frac{1}{\tau} y = \dot{u} \tag{1}$$

Taking the Laplace transform of equation (1) and assuming all initial conditions are zero, one obtains the first-order transfer function:

$$\frac{Y(s)}{U(s)} = H(s) = \frac{s}{s + \omega_c} \tag{2}$$

where $\omega_c = 1/\tau$ is the cutoff frequency.

Second-Order High-Pass Filter

Defining the second-order high-pass filter (SOHP) as:

$$\ddot{y} + 2\zeta\omega_n\dot{y} + \omega_n^2 y = \ddot{u} \tag{3}$$

and taking the Laplace transform of equation (3) (assuming all initial conditions are zero) yield the second-order transfer function

$$\frac{Y(s)}{U(s)} = \frac{s^2}{s^2 + 2\zeta\omega_n s + \omega_n^2} \tag{4}$$

MATHEMATICAL MODELS

The mathematical models to be considered are Euler's Integration, Zero-Order Hold, Bilinear Transformation, and Second-Order Adams-Bashforth Integration.

Euler's Integration

Euler's Integration is defined as:

$$y(n + 1) = y(n) + T\dot{y}(n) \tag{5}$$

First-order filter with Euler implementation- Applying equation (5) to (1) and taking the z-transform of the equation result in the transfer function:

$$H(z) = \frac{z - 1}{z + \omega_n T - 1} \tag{6}$$

Second-order filter with Euler implementation- The transfer function for the second-order high-pass filter (equation (3)) can be written as two differential equations:

$$\begin{aligned} \dot{x}_1 &= -2\zeta\omega_n x_1 - \omega_n^2 x_2 + u \\ \dot{x}_2 &= x_1 \end{aligned} \tag{7}$$

with the output equation as:

$$y = -2\zeta\omega_n x_1 - \omega_n^2 x_2 + u \tag{8}$$

Applying Euler's Integration and taking the z-transform, one obtains:

$$H(z) = \frac{z^2 + A_1 z + A_0}{z^2 + B_1 z + B_0} \tag{9}$$

where

$$\begin{aligned} A_0 &= 1 \\ A_1 &= -2 \\ B_0 &= 1 - 2\zeta\omega_n T + \omega_n^2 T^2 \\ B_1 &= 2(\zeta\omega_n T - 1) \end{aligned}$$

Zero-Order Hold

The z-transform of the ZOH implementation can be stated as:

$$H(z) = \frac{(z - 1)}{z} Z \left\{ \frac{H(s)}{s} \right\} \tag{10}$$

FOHP with ZOH implementation- Substituting equation (2) into (10), the z-transform of the FOHP becomes:

$$H(z) = \frac{z - 1}{z - e^{-\omega_c T}} \tag{11}$$

SOHP with ZOH implementation- Applying equation (10) to (4) yields:

$$H(z) = \frac{z^2 + A_1 z + A_0}{z^2 + B_1 z + B_0} \tag{12}$$

where

$$A_0 = Ge^{-k}$$

$$A_1 = -(1 + B_0)$$

$$B_0 = e^{-2k}$$

$$B_1 = -2e^{-k}\cos(m)$$

$$G = \cos(k) + (m/k)\sin(k)$$

$$k = \zeta\omega_n T$$

$$\ell = (\omega_n T)^2$$

$$m = \omega_n T\sqrt{1 - \zeta^2}$$

Bilinear Transformation

The z-transform for the Bilinear Transformation is defined as:

$$H(z) = H(s)\Big|_{s = \frac{2}{T}\ \frac{z-1}{z+1}} \tag{13}$$

FOHP using bilinear- Applying equation (13) to (2), we obtain the z-transform of the FOHP as:

$$H(z) = \frac{2(z - 1)}{(\omega_c T + 2)z + (\omega_c T - 2)} \tag{14}$$

SOHP using bilinear- Applying equation (13) to (4), one finds the z-transform of the SOHP to be:

$$H(z) = \frac{A_2 z^2 + A_1 z + A_0}{B_2 z^2 + B_1 z + B_0} \tag{15}$$

where

$$A_0 = A_2 = 4$$

$$A_1 = -8$$

$$B_0 = 4 - 4\zeta\omega_n T + (\omega_n T)^2$$

$$B_1 = -8 + 2(\omega_n T)^2$$

$$B_2 = 4 + 4\zeta\omega_n T + (\omega_n T)^2$$

Second-Order Adams-Bashforth Integration

The Second-Order Adams-Bashforth Integration is defined as:

$$y(n + 1) = y(n) + \frac{T}{2}[3\dot{y}(n) - \dot{y}(n - 1)] \tag{16}$$

The z-transform of equation (16) is:

$$H(z) = H(s)\Big|_{s = \frac{2z}{T}\quad\frac{z - 1}{3z - 1}} \tag{17}$$

FOHP using Adams-Bashforth Integration- If we substitute equation (2) into (17), we find the FOHP transfer function as:

$$H(z) = \frac{2z(z - 1)}{2z^2 + (3\omega_c T - 2)z - \omega_c T} \tag{18}$$

SOHP using Adams-Bashforth Integration- Substitution of equation (4) into (17) results in the SOHP transfer function:

$$H(z) = \frac{z^2(A_2 z^2 + A_1 z + A_0)}{B_4 z^4 + B_3 z^3 + B_2 z^2 + B_1 z + B_0} \tag{19}$$

where

$$A_0 = A_2 = 4$$

$$A_1 = -8$$

$$B_0 = (\omega_n T)^2$$

$$B_1 = 2[2\zeta\omega_n T - 3(\omega_n T)^2]$$

$$B_2 = 4 - 16\zeta\omega_n T + (3\omega_n T)^2$$

$$B_3 = 4(3\zeta\omega_n T - 2)$$

$$B_4 = 4$$

The z-transfer functions of the four mathematical models are summarized in table 1. Bode plots for each model were produced by evaluating these transfer functions at $z = e^{j\omega T} = \cos(\omega T) + j \sin(\omega T)$. The amplitude and phase of the steady-state response to a sinusoidal input are plotted as a function of normalized frequency (normalized to the natural frequency of the filter) for various normalized sample frequencies (parameters with units of samples per cycle at the natural frequency of the filter). The Bode responses of the associated continuous high-pass filters are included in the plots for comparison.

The normalized sample frequency is defined as:

$$n = \frac{\omega_s}{\omega_c} = \frac{2\pi}{T\omega_c}$$

for the FOHP, and

$$n = \frac{\omega_s}{\omega_n} = \frac{2\pi}{T\omega_n}$$

for the SOHP.

In the pole-location analyses, the poles of each model in table 1 are plotted as a function of $\omega_c T$ for the FOHP cases and $\omega_n T$ for the SOHP cases. For the SOHP cases, damping ratios of 0.3, 0.707, and 0.9 are representative of purposes of these analyses.

RESULTS

First-Order High-Pass Filter

Figures 1 through 4 present the Bode plots for the FOHP models. Based on the deviation from the desired continuous frequency response, the application of the Bilinear Transformation produced the best results over the sample frequency domain. All the mathematical models produced acceptable results when the normalized sample frequency (n) was greater than 50, or when the natural frequency times the sample period is less than or equal to 0.125 $[\omega_c T \leq (2\pi/50)]$. With the normalized sample frequency greater than 50, the gain deviation was within 1 dB and the phase was within 2° from the continuous FOHP for all mathematical models in the entire normalized frequency range up to the normalized Nyquist frequency of $\omega/\omega_c = n/2$.

Figures 5 through 8 show the pole locations of each model as a function of $\omega_c T$. Euler's Integration (fig. 5) becomes unstable when $\omega_c T \geq 2.0$. The Second-Order Adams-Bashforth (fig. 8) becomes unstable when $\omega_c T \geq 1.0$, which corresponds to $n \leq 6$. This is also shown in the phase plot of figure 4. In the limit, as $\omega_c T$ approaches infinity, the Bilinear pole goes to -1.0 and the ZOH pole goes to 0, which means that these two models give stable poles over the range of $\omega_c T$. Table 2 summarizes the value of $\omega_c T$ for marginally stable poles. These results are also applicable to first-order low-pass filter models.

The Bode plot for ZOH (fig. 2) shows a near-constant gain error across the frequency range for each sample rate. From the plot, one concludes that a DC gain must be calculated and applied to eliminate the error when using this model. The gain error is analyzed in appendix A and is found to be approximately equal to:

$$\text{gain error} = \left[1 + \left(\frac{7}{12}\,\frac{2\pi}{n} - 1\right)\frac{2\pi}{n}\right]^{-1/2}$$

Therefore, the ZOH model for FOHP should be:

$$H(z) = \frac{z - 1}{(\text{gain error})\left(z - e^{-\omega_c T}\right)}$$

Second-Order High-Pass Filter

Comparing figures 9 through 20 with the addition of the damping ratio (ζ) as another variable to the Bode plots, the Bilinear Transformation again produced the best overall results. With the normalized sample frequency greater than 50, the gain deviation was within 2.5 dB of the continuous SOHP for all mathematical models over the frequency range up to and including the appropriate Nyquist frequency. The phase deviation was within 9° of the continuous SOHP for all mathematical models except the ZOH model. However, the ZOH model was within 9° of the continuous SOHP when the normalized frequency was greater than 0.4. The ZOH results in figures 10, 14, and 18 show a gain adjustment can be calculated to compensate for the near-constant gain errors across the frequency spectrum, but this would not improve the phase errors.

Figures 21 through 24 show the pole locations of all four models versus $\omega_n T$. Euler's Integration (fig. 21) and Adams-Bashforth (fig. 24) show at what values of $\omega_n T$ the roots become unstable. These values of $\omega_n T$ relate to the normalized sample frequency (n) and to the increased phase deviations in the associated Bode plots. Table 3 summarizes the values of $\omega_n T$ for marginally stable poles. These results are also applicable to second-order low-pass filter models. Appendix B develops a stability check for Euler's Integration. Stable roots for SOHP using Euler's Integration will result if $\omega_n T \leq 2\zeta$.

CONCLUSION

The application of all four mathematical models to the linear first- and second-order high-pass filters reflects the dependence of the digital models on sample rate. As seen from the Bode plots, reasonable results can be obtained when the normalized sample frequency (n) is greater than 50. This sample frequency produced gain deviations within 1 dB and phase deviations within 2° of the associated continuous first-order high-pass filter output to a sinusoidal input. Gain deviations within 2.5 dB and phase deviations within 9° were obtained for the second-order high-pass filter except for the ZOH model at low normalized frequencies. The pole-location analyses show the Bilinear Transformation and ZOH models yield stable poles for all practical natural frequencies and calculation rates. Based on frequency response and pole-location analyses, Euler's Integration and Adams-Bashforth models should both be used with caution. The Bilinear Transformation model gave the best overall results over the entire frequency range up to the Nyquist frequency and is recommended for both high-pass filter cases.

Ames Research Center
National Aeronautics and Space Administration
Moffett Field, Calif. 94035, September 15, 1980

APPENDIX A

APPARENT GAIN ON ZOH FIRST-ORDER HIGH-PASS FILTER

The Bode plot for the FOHP using ZOH (fig. 2) shows a near constant gain across the frequency range as a function of sample rate. The following analysis is an effort to find a compensation for the apparent gain error.

ZOH Model

The transfer function for the ZOH first-order high-pass filter model is:

$$H(z) = \frac{z - 1}{z - e^{-\omega_c T}}$$

The frequency response equation is obtained by substituting the relationship:

$$z = e^{j\omega T} = e^{j\left(\frac{2\pi}{n}\frac{\omega}{\omega_c}\right)} = \cos\left(\frac{2\pi}{n}\frac{\omega}{\omega_c}\right) + j\,\sin\left(\frac{2\pi}{n}\frac{\omega}{\omega_c}\right)$$

in the transfer function. If $a = 2\pi/n$ and $b = \omega/\omega_c$, the equation is:

$$H(e^{j\omega T}) = \frac{\cos(ab) - 1 + j\,\sin(ab)}{\cos(ab) - e^{-a} + j\,\sin(ab)}$$

The magnitude squared is:

$$|H|^2 = \frac{2[1 - \cos(ab)]}{1 - 2e^{-a}\cos(ab) + e^{-2a}}$$

Taking the series expansion of each term to the fifth power and combining the terms result in the equation:

$$|H|^2 = \frac{b^2[1 - (b^2/12)]}{(1 - a)(1 + b^2) + (7/12)a^2 + a^4b^2\{(1/2)[1 - (b^2/6)] - (a/6)[1 - (b^2/2)]\}}$$

If $b < 1$, the magnitude squared is:

$$|H|^2 = \frac{b^2}{(1 - a) + (7/12)a^2 + (a^4b^2/12)[6 - b^2 - a(2 - b^2)]}$$

Therefore, for small b, the magnitude is

$$|H| = \left(\frac{b^2}{1 - a + (7/12)a^2}\right)^{1/2}$$

Continuous Case

The transfer function for the continuous case is:

$$H(s) = \frac{\tau s}{\tau s + 1}$$

Let

$$s = j\omega T$$

and

$$\tau = \frac{1}{\omega_c}$$

and the frequency response becomes

$$H(j\omega T) = \frac{j(\omega T/\omega_c)}{j(\omega T/\omega_c) + 1}$$

$$= \frac{jb}{jb + 1}$$

The magnitude is:

$$|H|^2 = \frac{b^2}{b^2 + 1}$$

or

$$|H| = \frac{b}{\sqrt{b^2 + 1}}$$

Therefore, for $b << 1$,

$$|H| \simeq b$$

Comparing the magnitudes of the ZOH and continuous case results in:

$$\text{gain error} = \left[1 - \frac{2\pi}{n} + \frac{7}{12}\left(\frac{2\pi}{n}\right)^2\right]^{-1/2}$$

The gain error is a function of the normalized sample frequency (n), if normalized frequency (b) is less than unity. Therefore, to correct the gain error in the ZOH FOHP, the transfer function should be:

$$H(z) = \frac{(\text{gain})(z - 1)}{z - e^{-\omega_c T}}$$

where

$$\text{gain} = \frac{1}{\text{gain error}}$$

APPENDIX B

EULER'S INTEGRATION — STABILITY CHECK FOR SOHP

This appendix derives a simple check for stability when applying Euler's Integration on a SOHP. The transfer function for SOHP using Euler's Integration is:

$$H(z) = \frac{z^2 - 2z + 1}{z^2 + 2(\zeta\omega_n T - 1)z + (1 - 2\zeta\omega_n T + \omega_n^2 T^2)}$$

After factoring, the denominator is:

$$[z + (\zeta\omega_n T - 1) + j\omega_n T\sqrt{1 - \zeta^2}\,][z + (\zeta\omega_n T - 1) - j\omega_n T\sqrt{1 - \zeta^2}]$$

For stability, the magnitude of the vector Z must be less than or equal to unity ($|z| \leq 1$). Therefore,

$$[(\zeta\omega_n T - 1)^2 + (\omega_n T\sqrt{1 - \zeta^2})^2]^{1/2} \leq 1$$

which reduces to $\omega_n T < 2\zeta$ for stable roots. This relationship is also applicable when applying Euler's Integration to a second-order low-pass filter because the characteristic equation for both filters is the same.

REFERENCES

1. Franklin, Gene F.; and Powell, David J.: Digital Control of Dynamic Systems. Addison-Wesley Publishing Co., Inc., 1980.

2. D'Azzo, John J.; and Houpis, Constantine H.: Feedback Control System Analysis and Synthesis. Second Ed., McGraw-Hill Book Co., Inc., 1966.

TABLE 1.- Z-TRANSFER FUNCTIONS OF THE FOUR MODELS

Models	FOHP	SOHP
Euler's Integration	$\frac{(z - 1)}{z + (\omega_c T - 1)}$	$\frac{z^2 - 2z + 1}{z^2 + 2(k - 1)z + (1 - 2k + \ell)}$
Zero-Order Hold	$\frac{(z - 1)}{z - e^{-\omega_c T}}$	$\frac{z^2 - [2e^{-k}\cos(m)]z - e^{-2k}}{z^2 - (1 + Ge^{-k})z + Ge^{-k}}$
Bilinear Transformation	$\frac{2(z - 1)}{(2 + \omega_c T)z + (\omega_c T - 2)}$	$\frac{4z^2 - 8z + 4}{(4 + 4k + \ell)z^2 - (8 - 2\ell)z + 4 - 4k + \ell}$
Second-Order Adams Bashforth	$\frac{2z(z - 1)}{2z^2 + (3\omega_c T - 2)z - \omega_c T}$	$\frac{4z^2(z^2 - 2z + 1)}{4z^4 + (12k - 8)z^3 + (4 - 16k - 9\ell)z^2 + (4k - 6\ell)z + \ell}$

where

$G = \cos(k) + (m/k)\sin(k)$

$k = \zeta\omega_n T$

$\ell = (\omega_n T)^2$

$m = \omega_n T \sqrt{1 - \zeta^2}$

TABLE 2.- FOHP $\omega_c T$ VALUE FOR MARGINALLY STABLE POLES

Math model	$\omega_c T$
Euler	2.0
ZOH	None
Bilinear	Infinity
Adams-Bashforth	1.0

TABLE 3.- SOHP $\omega_c T$ VALUES FOR MARGINALLY STABLE POLES

Math model	$\omega_n T$		
	$\zeta = 0.3$	$\zeta = 0.707$	$\zeta = 0.9$
Euler[a]	0.6	1.41	1.8
ZOH	None	None	None
Bilinear	Infinity	Infinity	Infinity
Adams-Bashforth	0.84	0.95	0.99

[a]Stable poles for Euler's Integration can be calculated using the relationship $\omega_n T \leq 2\zeta$.

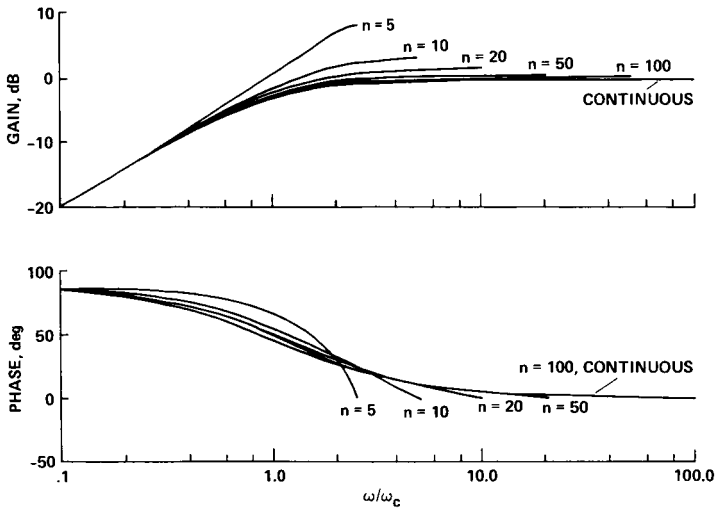

Figure 1.- Bode plot for first-order high-pass filter using Euler's Integration.

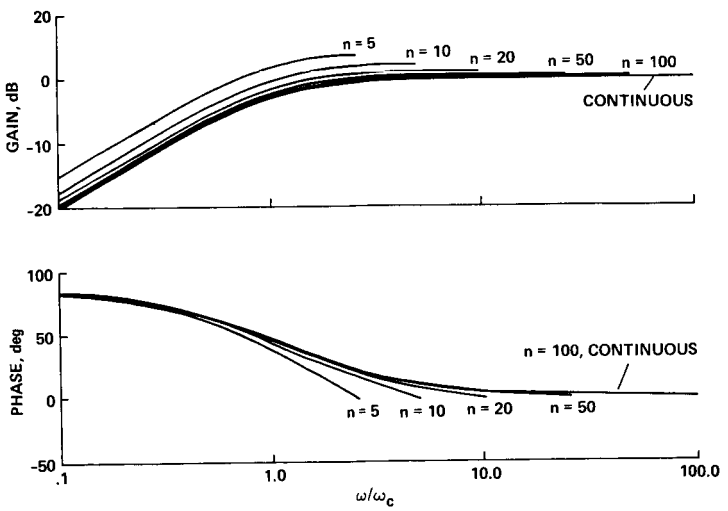

Figure 2.- Bode plot for first-order high-pass filter using zero-order hold.

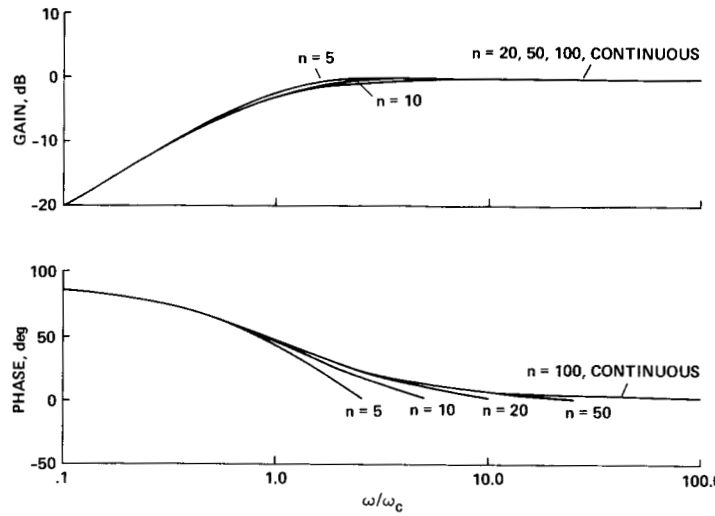

Figure 3.- Bode plot for first-order high-pass filter using Bilinear Transformation.

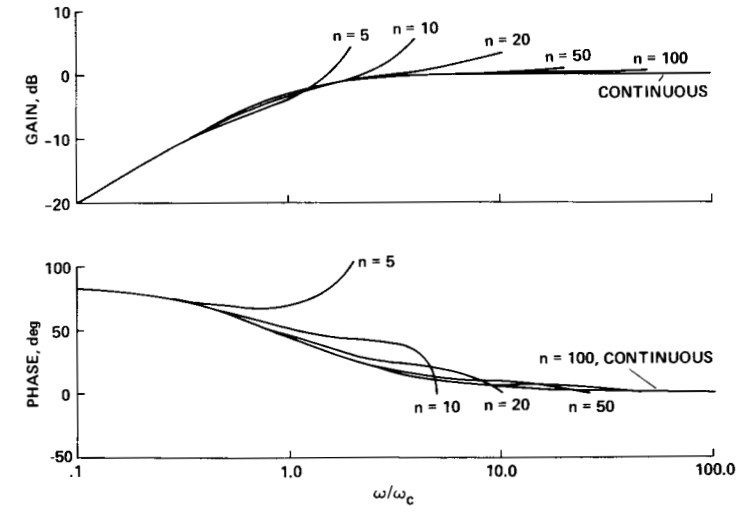

Figure 4.- Bode plot for first-order high-pass filter using Adams-Bashforth.

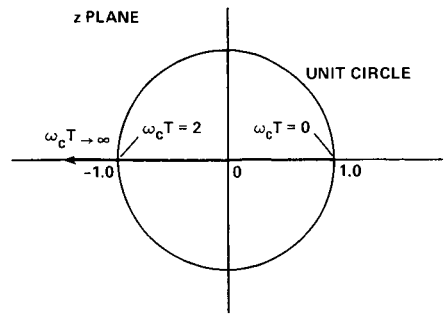

Figure 5.- Euler's integration FOHP pole location.

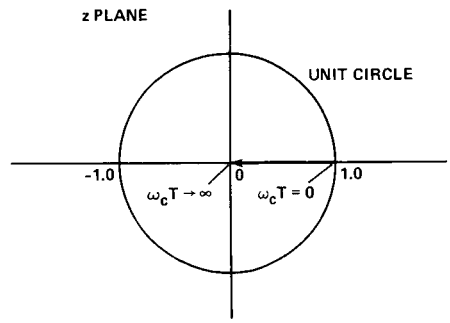

Figure 6.- Zero-order hold FOHP pole location.

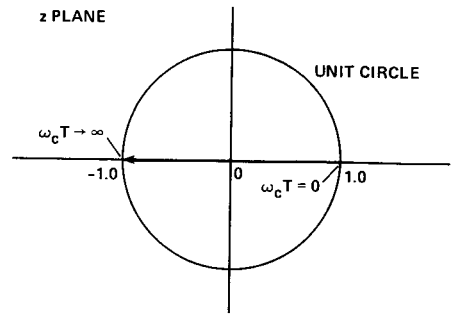

Figure 7.- Bilinear Transformation FOHP pole location.

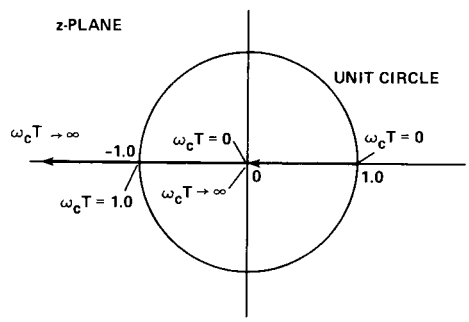

Figure 8.- Second-Order Adams-Bashforth FOHP pole location.

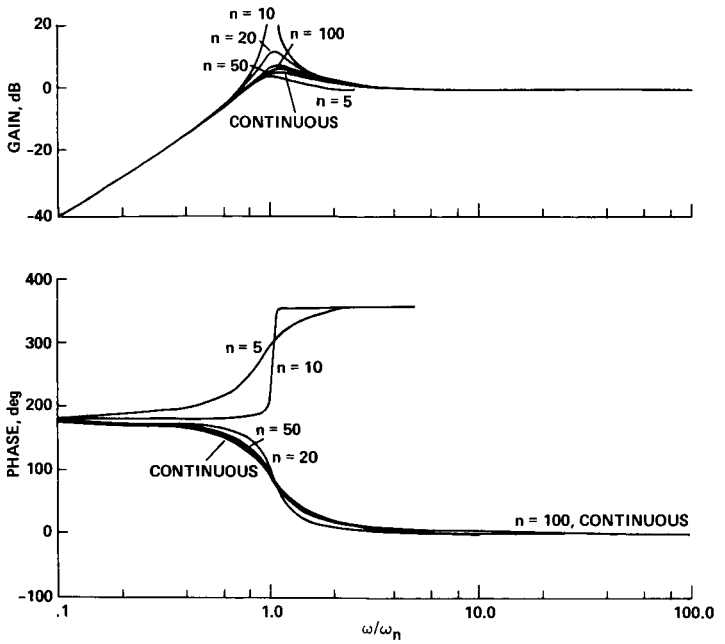

Figure 9.- Bode plot for second-order high-pass filter using Euler's Integration; $\zeta = 0.3$.

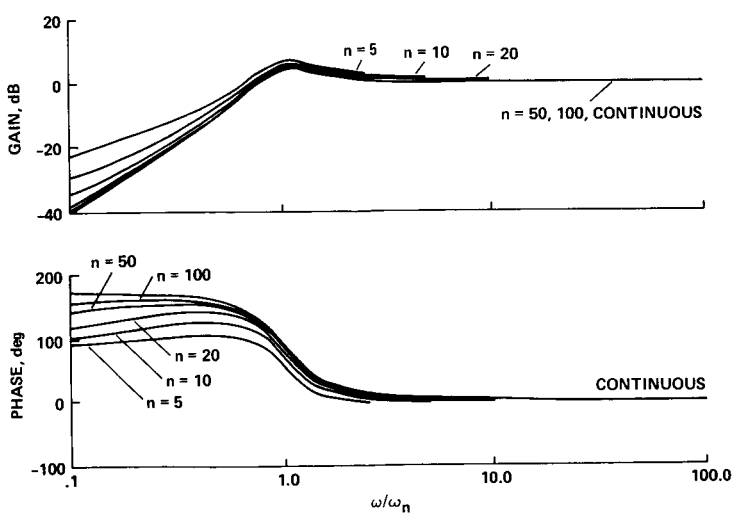

Figure 10.- Bode plot for second-order high-pass filter using zero-order hold; $\zeta = 0.3$.

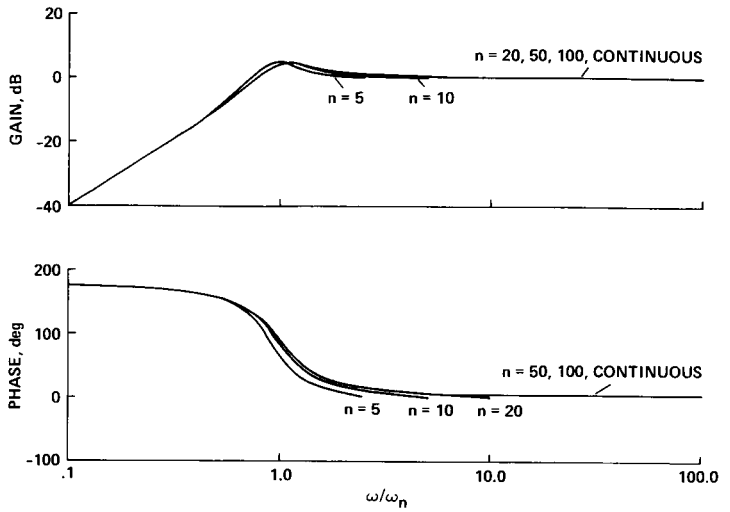

Figure 11.- Bode plot for second-order high-pass filter using Bilinear Transformation; $\zeta = 0.3$.

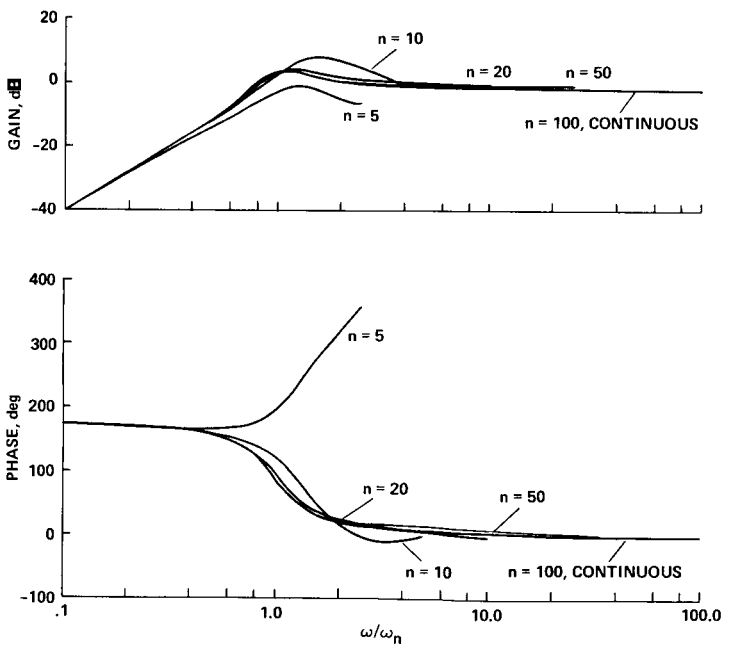

Figure 12.- Bode plot for second-order high-pass filter using Adams-Bashforth; $\zeta = 0.3$.

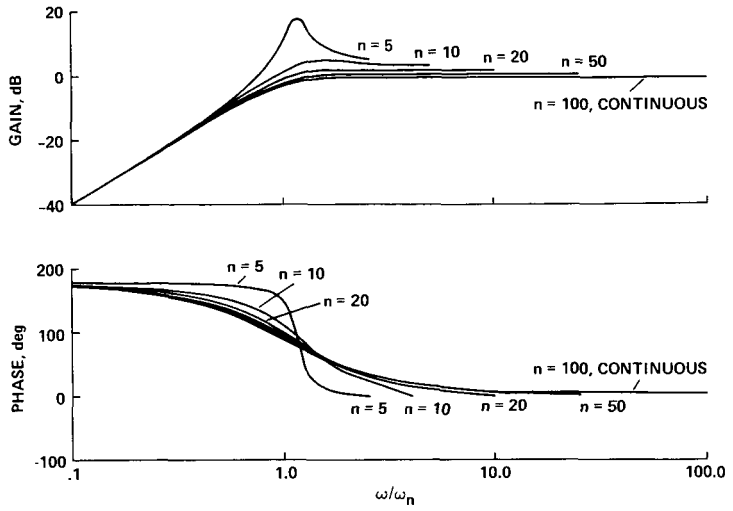

Figure 13.- Bode plot for second-order high-pass filter using Euler's Integration; $\zeta = 0.707$.

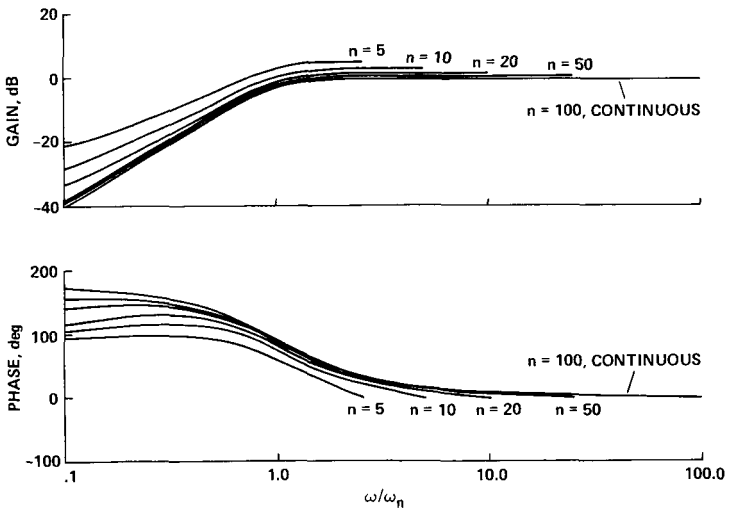

Figure 14.- Bode plot for second-order high-pass filter using zero-order hold; $\zeta = 0.707$.

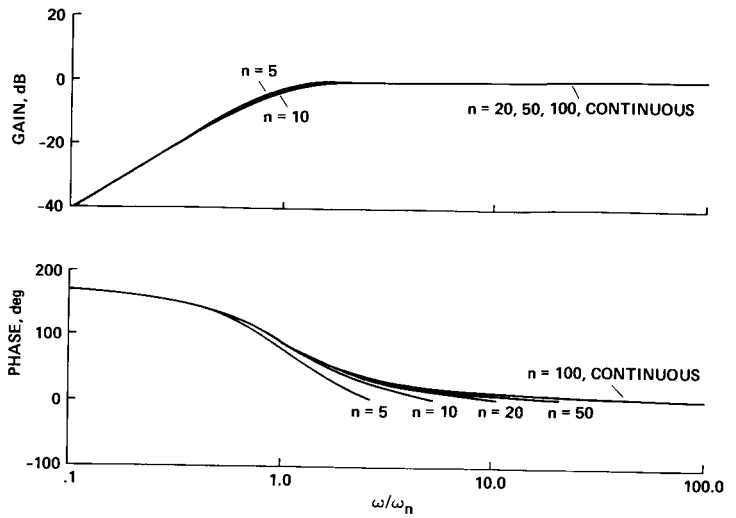

Figure 15.- Bode plot for second-order high-pass filter using Bilinear Transformation; $\zeta = 0.707$.

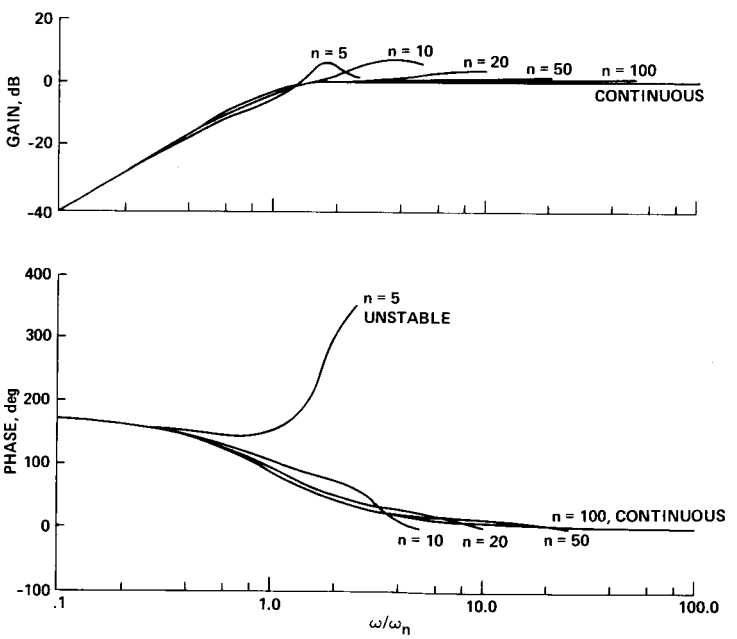

Figure 16.- Bode plot for second-order high-pass filter using Adams-Bashforth Integration; $\zeta = 0.707$.

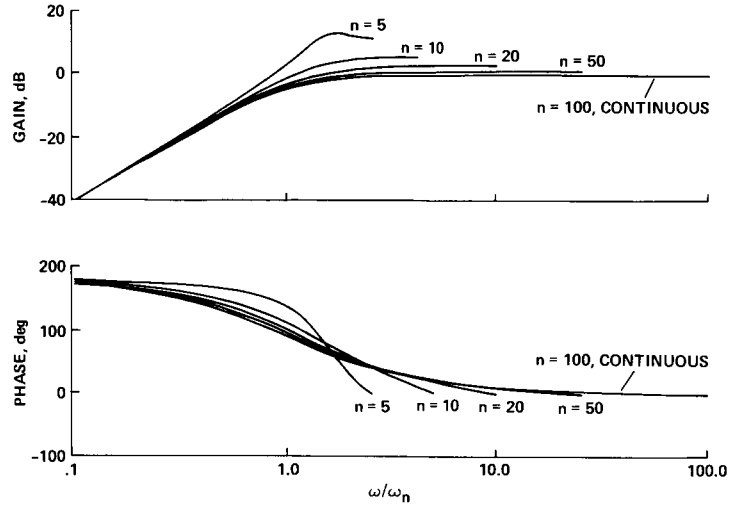

Figure 17.- Bode plot for second-order high-pass filter using Euler's Integration; $\zeta = 0.9$.

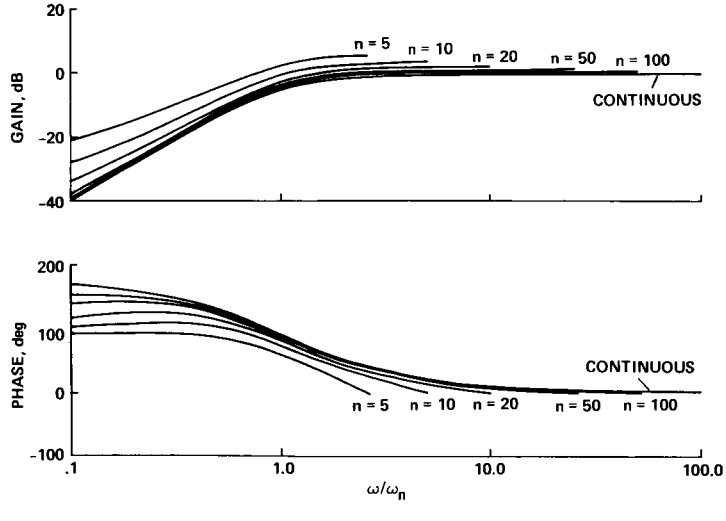

Figure 18.- Bode plot for second-order high-pass filter using zero-order hold; $\zeta = 0.9$.

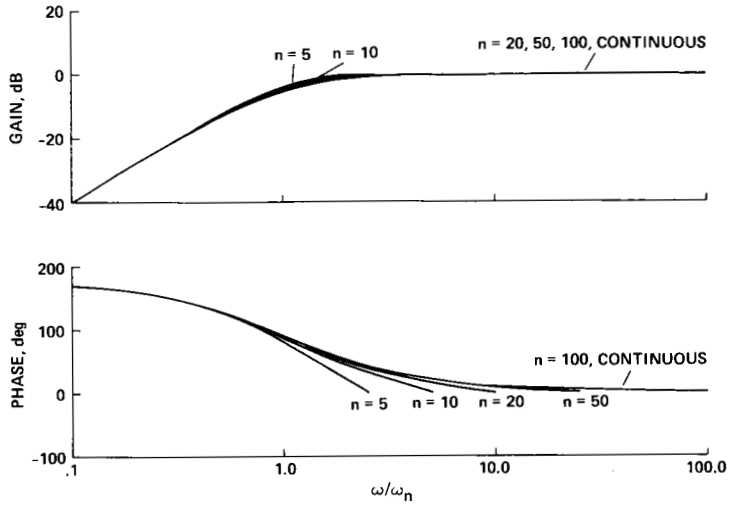

Figure 19.- Bode plot for second-order high-pass filter using Bilinear Transformation; $\zeta = 0.9$.

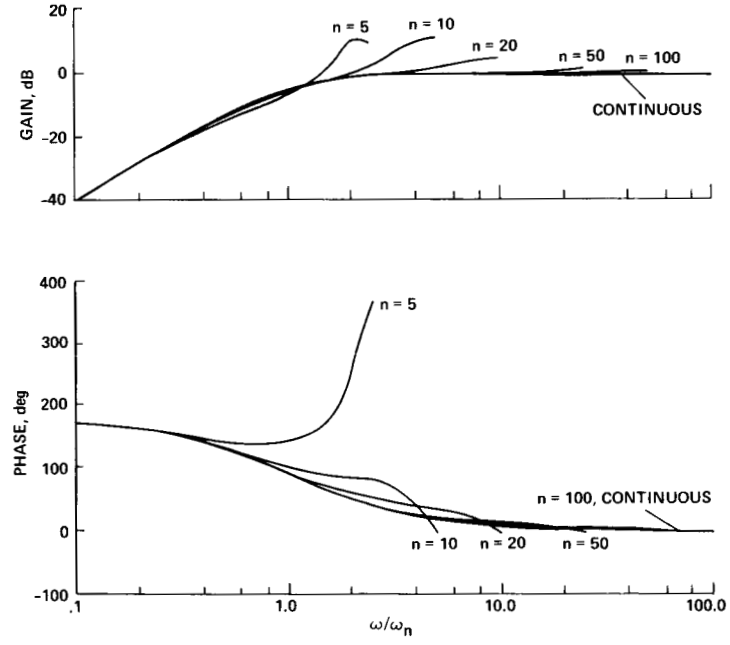

Figure 20.- Bode plot for second-order high-pass filter using Adams-Bashforth Integration; $\zeta = 0.9$.

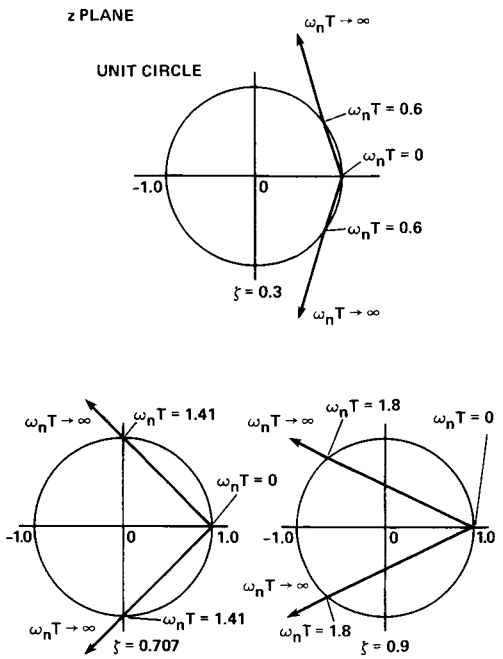

Figure 21.- Euler's Integration SOHP pole location.

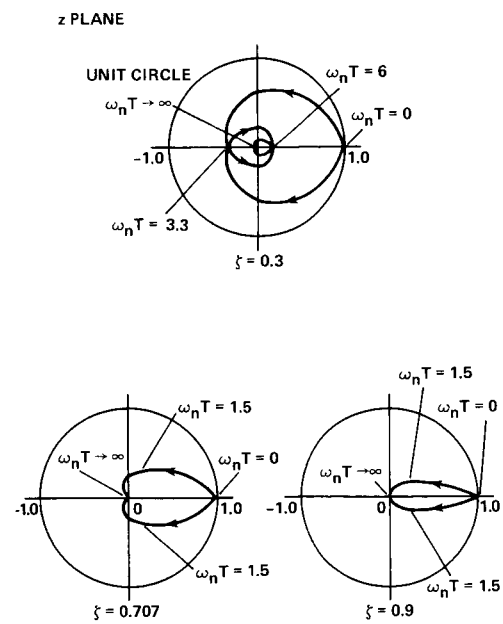

Figure 22.- Zero-order hold SOHP pole locations.

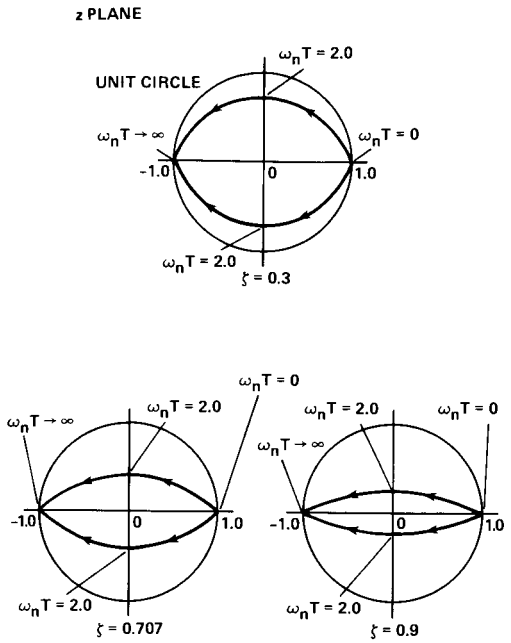

Figure 23.- Bilinear Transformation SOHP pole location.

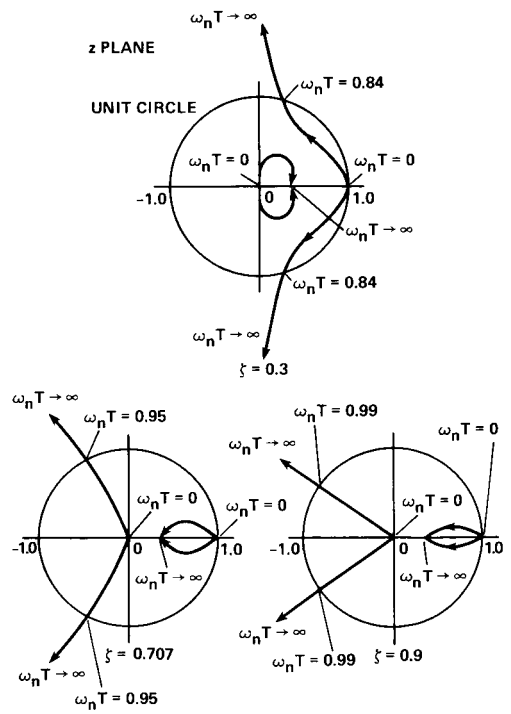

Figure 24.- Second-order Adams Bashforth SOHP pole location.

1. Report No.	2. Government Accession No.	3. Recipient's Catalog No.
NASA TP-1797		

4. Title and Subtitle	5. Report Date
SAMPLE DATA EFFECTS OF HIGH-PASS FILTERS	January 1981
	6. Performing Organization Code

7. Author(s)	8. Performing Organization Report No.
David O. Chin	A-8361
	10. Work Unit No.
9. Performing Organization Name and Address	505-36-31
Ames Research Center, NASA Moffett Field, CA 94035	11. Contract or Grant No.
	13. Type of Report and Period Covered
12. Sponsoring Agency Name and Address	Technical Paper
National Aeronautics and Space Administration Washington, D.C. 20546	14. Sponsoring Agency Code

15. Supplementary Notes

16. Abstract

The fact that aircraft motion simulators inherently have less travel than the actual aircraft being simulated has resulted in the application of digital washout filters in the computer software. Four commonly used mathematical models of linear first- and second-order high-pass washout filters were analyzed. These models were Euler's Integration, Zero-Order Hold, Bilinear Transformation, and Second-Order Adams-Bashforth Integration. Bode responses for each model at various sample rates were compared to the continuous filter response. The results show that higher sample rates produce Bode responses approaching the continuous response and the Bilinear Transformation model produced the best responses over the frequency spectrum and sample rates. Pole location analysis of each model in the z-plane shows the Bilinear Transformation and Zero-Order Hold models gave stable poles regardless of time step size, whereas the other models did not always display stable poles.

A near constant gain error over the entire frequency spectrum was discovered in the Zero-Order Hold cases and a correction gain was calculated for the first-order high-pass filter case.

17. Key Words (Suggested by Author(s))	18. Distribution Statement
Sample data effects High-pass filter Digital filter	Unclassified - Unlimited Subject Category 05

19. Security Classif. (of this report)	20. Security Classif. (of this page)	21. No. of Pages	22. Price*
Unclassified	Unclassified	30	A03

*For sale by the National Technical Information Service, Springfield, Virginia 22161

NASA-Langley, 1981